

Solar accessibility in developing cities: A case study in Kowloon East, Hong Kong



Rui Zhu^a, Linlin You^{b,c,*}, Paolo Santi^{d,e}, Man Sing Wong^f, Carlo Ratti^d

^a Future Urban Mobility IRG, Singapore-MIT Alliance for Research and Technology, 1 Create Way, 09-02 Create Tower, Singapore 138062, Singapore

^b College of Computer Science and Software Engineering, Shenzhen University, 3688 Nanhai Ave, Nanshan Qu, Shenzhen 518060, China

^c Intelligent Transportation Systems Lab, Massachusetts Institute of Technology, Cambridge, MA 02139, USA

^d Senseable City Laboratory, Massachusetts Institute of Technology, Cambridge, MA 02139, USA

^e Istituto di Informatica e Telematica del CNR, 56124 Pisa, Italy

^f Department of Land Surveying and Geo-Informatics, The Hong Kong Polytechnic University, 181 Chatham Road South, Kowloon, Hong Kong

ARTICLE INFO

Keywords:

Solar urban planning
Solar accessibility
Urban morphology
3D cities

ABSTRACT

Solar accessibility, defined as the solar irradiation received in a spatial and temporal domain, is increasingly becoming a practical demand in a variety of applications, especially in dense and high-rise urban areas where people prefer natural daylighting accommodations and offices and enterprises desire rooftops with high exposure to sun for photovoltaic cells. However, new buildings may substantially alter spatio-temporal solar distribution and obstruct exposure to solar power significantly. Thus, providing an accurate quantification of how solar accessibility is impacted by a developing urban environment is a key step in the development of sustainable cities. Motivated by this observation, a solar irradiation estimation model has been designed, which allows solar radiation from a particular elevation and azimuth to pass through urban surfaces modelled as 3D polygons, resulting in the creation of 3D shadow surfaces. As such, the urban surfaces can also be represented as 3D point clouds of irradiations determined by both solar radiation and shadow. By applying the model to existing and planned urban environment, it is possible to estimate the transformation of solar accessibility at the district scale. As a case study, a master plan for the Kowloon East district proposed by the Hong Kong government has been considered, and an application of the propose methodology found that new buildings to be built in the district can obtain considerable solar energy, while having a marginal impact on existing buildings. This case study suggests that the model can be used in many other cities for a variety proposes.

1. Introduction

With growing urbanization rate, especially in the developing countries, buildings and infrastructures are being built at a very fast pace. Changes of urban morphology may significantly impact the spatio-temporal distribution of solar energy in the city. This transformation may substantially impact various solar applications: photovoltaic cells need large solar irradiations to generate electricity (Chu & Majumdar, 2012; GEA Writing Team, 2012; Ma, Goldstein, Pitman, Haghadi, & MacGill, 2017; Molina, Falvey, & Rondanelli, 2017); offices are recommended to have substantial daylight and tend to have moderate sunshine (Wong, 2017); pedestrians tend to follow thermal comfort routings under the shadow (Middel, Lukasczyk, & Maciejewski, 2017), and so on. In addition, a change of urban morphology may exacerbate the urban heat island phenomenon because of the heat accumulation coming from solar irradiations (Aflaki et al., 2017; Masson,

Bonhomme, Salagnac, Briottet, & Lemonsu, 2014). Therefore, the issue of solar accessibility and its transformation as an effect of changes in the built environment have attracted significant public attention.

Several studies that consider solar accessibility and its relationship with the development of sustainable cities have already been conducted in urban planning community. In order to design energy efficient cities, the impact of utilizing photovoltaic potential was investigated in the aspects of economy by considering the relation between consumption and supply of solar energy (Amado & Poggi, 2014; Amado, Poggi, & Amado, 2016; Vakilifard, Bahri, Anda, & Ho, 2019), urban environment by estimating the reduction of air-pollution emission (Nastasi & Di Matteo, 2016), and policy by proposing feed-in tariffs (Poroschi & Ambrey, 2019).

Since geographic modelling is needed to understand the dynamic urban environment (Lin et al., 2013; Lu et al., 2019), other studies determined the optimal geometry of buildings in the context of urban

* Corresponding author at: College of Computer Science and Software Engineering, Shenzhen University, 3688 Nanhai Ave, Nanshan Qu, Shenzhen 518060, China.
E-mail address: linlin@smart.mit.edu (L. You).

morphology, considering metrics such as building massing, density, and orientation (Kanters, Wall, & Dubois, 2014; Lobaccaro & Frontini, 2014; Morganti, Salvati, Coch, & Cecere, 2017; Savvides, Vassiliades, Michael, & Kalogirou, 2019), in order to provide an efficient solar urban planning. Particularly, one study proposed 12 building block configurations and manipulated three geometrical parameters (the width of streets, the heights of existing and planned buildings, and the massing of buildings) to adjust building layouts and finally to obtain an optimal integration (Savvides et al., 2019). However, an optimal solution proposed in an ideal scenario may not be able to apply in real urban environment straightforwardly since planned buildings may be adjusted by other influential factors comprehensively, such as noisy control, indoor day-lighting time, and traffic dispersion.

Therefore, understanding the effect of a transformed urban morphology on solar accessibility of existing and planned buildings is also imperative, if a master plan of buildings has been established. This can be done with the comparison between buildings in the current and future city (Lauka, Haine, Gusca, & Blumberga, 2018; Lobaccaro & Frontini, 2014). The two studies discussed the changes of solar accessibility if new buildings are built up, which only focused on a limited number of buildings and the changes in different partitions of buildings were unknown. In comparison, our study aims to investigate the transformation of solar accessibility both locally and globally in space, covering a large urban area.

In order to investigate transformation of solar accessibility in a dense urban area over the spatial and temporal domain, an estimation of solar irradiations on a three-dimensional (3D) city is going to be presented. Here, a city is represented as a set of 3D point clouds enriched with solar irradiation information. The model proposed herein provides three contributions with respect to state of the art. First, shadows are created accurately taking *all* buildings in the study area into consideration, which is particularly important for cities having numerous high-rise buildings. Second, the model supports various building geometries, where footprints of buildings are concave polygons and one polygon may contain one or more polygons. Third, it supports big-data computation with a large number of buildings, which facilitates large scale master planning.

The rest paper is organized as follows. Section 2 provides a literature review on modelling of a three-dimensional solar city and empirical investigation. Section 3 defines the concepts of solar accessibility and its transformation, followed by a methodology to model a three-dimensional solar city in Section 4. Section 5 then presents an empirical investigation. Finally, in Section 6, we draw the discussion and conclusion.

2. Literature review

2.1. Modelling of a three-dimensional solar city

In order to investigate the solar transformation, it is important to estimate photovoltaic potential accurately. Some studies incorporated sky view factors for the estimation of photovoltaic potential (Gong, Zeng, Ng, & Norford, 2019; Polo L'peza, Salab, Tagliabuec, Frontinia, & Bouziri, 2016), which essentially considered footprints and heights of the surrounding buildings. However, it only focuses on street canyons and irradiations on buildings cannot be obtained. Some only focused on rooftops (Izquierdo, Montañés, Dopazo, & Fueyo, 2011; Jakubiec & Reinhart, 2013; Li, Ding, Liu, & Wang, 2016; Wong et al., 2016). Specifically, one study incorporated the probability distribution of annual cloud cover to generate a solar potential map on rooftops (Wong et al., 2016). Similarly, our study will also utilize historical cloud cover data to determine the irradiation of direct incoming solar radiation more reliably.

Further studies estimated solar energy on façades and the ground (Chatzipoulka, Compagnon, & Nikolopoulou, 2016), or façades and rooftops (Catita, Redweik, Pereira, & Brito, 2014; Liang, Gong, Li, &

Ibrahim, 2014; Liang, Gong, Zhou, Ibrahim, & Li, 2015; Redweik, Catita, & Brito, 2013). For example, Catita et al. (2014) developed the SOL algorithm to generate hyperpoints on façades (2.5D vertical surfaces) to present solar radiations. Liang et al. (2014, 2015) focused on the visualization of irradiations at an instant of time as 2D raster maps transformed from 3D surfaces, which essentially is an extension of well-established 2D r.sun model. Thus, the main contribution is on visualization as it achieves real-time rendering by using the graphics processing unit (GPU) technique. In a different aspect, the effect of greenery on the amount of solar energy received on building envelopes was considered (Lindberg, Jonsson, Honjo, & Wästberg, 2015), which is vital for some cities where greenery is dominant. However, greenery will not be considered in our model since the main focus of this study is the shadow effect of future constructed buildings in dense urban areas, where greenery effect becomes less important.

A few studies indicated the capability of estimating solar irradiation on all the partitions of rooftops, façades, and ground simultaneously (Erdélyi, Wang, Guo, Hanna, & Colantuono, 2014; Hofierka & Zlocha, 2012; Lindberg et al., 2015; Lobaccaro, Carlucci, Croce, Paparella, & Finocchiaro, 2017). For instance, the v.sun module considered shadow effect caused by surrounding buildings and estimated 3D solar irradiation, which was implemented based on the r.sun model that enables the computation of segmenting 3D vectors to smaller polygons (Hofierka & Zlocha, 2012). In another study, the SORAM model used a ray-tracing algorithm and refined the Perez, Ineichen, Seals, Michalsky, and Stewart (1990) model to determine whether a 3D ray vector intersects with a voxel and to calculate solar irradiations on building surfaces (Erdélyi et al., 2014). However, the capability of applying these models to a large urban area is not clear, and it becomes even uncertain when buildings have complex geometries.

Comparing with Catita et al. (2014), our study will propose a similar approach that depicts 3D urban envelopes as spatially contiguous 3D point clouds to present solar irradiations on *all* the three partitions. Similar with Erdélyi et al. (2014) and Hofierka and Zlocha (2012), we will develop an algorithm to make 3D intersections between irradiations and 2.5D buildings, which will consider *all* the irradiations intersecting with *all* the buildings allowing complex geometries. In this case, shadow effect caused by far-away buildings can also be considered, which is particularly important for urban areas possibly having numerous high-rise buildings. In addition, the model will be developed in a spatial database management system to allow fast computation.

2.2. Empirical investigation

Empirical investigation conducted in the previous studies may be categorized into two, i.e., solar changes on the existing buildings versus solar transformations comparing with the existing and planned buildings. For example, one study investigated spatial and quantitative variation of monthly irradiation on a single façade (Catita et al., 2014). In a more aggregated level, Peronato, Rey, and Andersen (2018) analysed solar irradiation on a cluster of buildings at different spatial and temporal granularities (e.g., individual surfaces or buildings over hours) in a high-density urban area. Considering seasonal variation, Lindberg et al. (2015) compared hourly irradiations on rooftops and façades on two days respectively in two different seasons (winter versus spring), which incorporated the influence of vegetation. Another study found that hourly mean solar irradiation over 12 months in Trondheim varied dramatically, suggesting significant seasonal influence in a high latitude (Lobaccaro et al., 2017). In a more advanced aspect, this study highlighted solar irradiations which were increased or decreased comparing with the solar urban planning recommendations. It also obtained increased solar irradiations by optimizing façade orientations in a master plan. However, the above studies do not quantitatively depict the transformation of solar irradiations on *all* the partitions. To better understand the influence of transformed urban morphology when new buildings are built, our study will also make comparisons

between the ‘current’ and the ‘future’ city on different partitions over various temporal scales.

3. Definition of solar accessibility

Solar accessibility is defined as the irradiation of solar radiation u received by a unit of floor area a_u during a period of time t_p . With the development of a city, three scenarios can happen: some buildings are maintained, some are destroyed, and some new buildings are constructed. Trajectory of solar radiation can change with the transformation of a city, leading to the modification of the irradiation from u to u' in the same a_u and t_p . In order to investigate the changes, the concept of *transformation of the solar accessibility* denoted by $u_{sa} = (u' - u)$ is thus introduced. According to the definition, a value of u_{sa} larger than 0 is usually preferred for the purpose of receiving as much solar energy as possible. An urban planning strategy that aims at keeping u_{sa} above zero would define what can be considered a sustainable urban development. Particularly, more detailed investigation can be conducted for the maintained buildings, moving from the floor area a_u to exterior urban surfaces $\{g\}$ located on a_u , which includes rooftops and wall façades.

4. Modelling of a three-dimensional solar city

A simple and effective modelling strategy is proposed in order to construct a three-dimensional (3D) solar city. Given 2D polygons of buildings enriched with height information, 3D exterior urban surfaces can be built as a set of polygons and denoted by \mathcal{G} . Then, each urban surface $g \in \mathcal{G}$ is discretized as spatially contiguous and homogeneous grid cells at a static resolution of d , so that 3D point clouds denoted by \mathcal{P} can be constructed at the center of each grid cell in each urban surface to represent exterior urban surfaces. Specifically, $\mathcal{P} = \{p\}$ and $p = \langle id, g, l, u \rangle$, which means that a point p uniquely identified by id is located on the surface of g with an absolute location l and a quantified irradiation u . Meanwhile, a set of parallel solar radiation lines can be determined and represented by $\mathcal{R} = \{r\}$, where $r = \langle e, z, t, l, u \rangle$ denotes that direct solar radiation r passes through the atmosphere and approaches the land surface from an elevation e and azimuth z at instant of time t and location l with an irradiation u . Hence, 3D shadow surfaces recorded as $\mathcal{S} = \{s\}$ can be produced by making 3D intersections between \mathcal{G} and \mathcal{R} , where s is a 3D polygon associated with a façade of a building. Furthermore, points in \mathcal{P} can be determined in brightness or in shadow if they are above or below the shadow surfaces, respectively.

An urban surface can be more specifically represented by $g(i, j \in \mathbb{Z})$, which denotes a façade surface of a building i indexed by j if $(i > 0 \wedge j > 0)$, a rooftop surface if $(i > 0 \wedge j = 0)$, or a ground surface if $(i = 0 \wedge j = 0)$. Thus, two parallel solar radiation lines passing through two consecutive vertexes of the rooftop will intersect on the ground as another two vertexes, such that an initial 3D parallelogram

can be built from the four vertexes to represent a shadow surface $s(i, j)$ (Fig. 1a). However, $s(i, j)$ may intersect with some façades of the same building or with rooftops and/or façades of other buildings before arriving at the ground. Thus, we need to modify the model in order to make the definition of $s(i, j)$ physically realistic.

Let a complete set of line segments made by intersections between $s(i, j)$ and rooftops and façades of buildings be recorded as $Q = \{q\}$. Then, solar radiation lines passing through the two vertexes of q will also intersect at the ground as another two vertexes, so that a 3D parallelogram can also be made and represented by s_q . Further, a complete set of s_q made from Q , which corresponds to the $s(i, j)$, can be spatially unified as a single polygon denoted by s_Q (Fig. 1b). On top of this, a physically correct 3D shadow surface having considered interruptions of other buildings can be obtained and recorded as $s^*(i, j)$ by cutting off s_Q from $s(i, j)$, i.e. $s^*(i, j) = s(i, j) - s_Q$.

Therefore, a complete set of 3D shadow line segments produced from the intersections between $\{s^*(i, j)\}$ and urban surfaces \mathcal{G} can be obtained and represented by $Q^* = \{q^*\}$. If a set of point clouds and q^* are in the same façade $g(i, j)$ and these point clouds are below q^* in an orthographic projection, then the set of the point clouds are under the shadow. In the other scenario, if a set of point clouds are on rooftop or ground surfaces, and footprints of the point clouds are in a 2D polygon $s^*(i, j)$ made from the orthographic projection of $s^*(i, j)$, then the set of the point clouds are also under the shadow. Otherwise, point clouds are considered to be in brightness.

Given the irradiation u generated by solar radiation r , and a cloud point p in brightness and on a rooftop or ground surface, the irradiation u' received by p is computed as $u' = u \sin(e)$ according to the energy conservation law (Fig. 1c). Similarly, u' is computed as $u' = u \cos(e) \sin(\Delta z)$ for p in brightness and on a façade surface, where Δz is the difference between z and z' , in which z' is the azimuth of the façade facing at. At this step, irradiations of all the point clouds received from direct incoming solar radiation r can be updated accordingly.

5. Empirical investigation

5.1. Study area

Hong Kong has a population of over seven million with only a limit of 269 km² built-up area (Planning Department, 2017), which makes it one of the most dense and high-rise cities across the world. In order to accelerate sustainable development of Hong Kong, the government has proposed an Energizing Kowloon East (EKE) initiative to transform Kowloon East into a core business district, where a number of office blocks and residential buildings are to be built in the recent years (Development Bureau, 2019). The study focuses on the Kai Tak region covering an area of 2.75 km² (Fig. 2a), which is the core area for the development of EKE, and this area and the number of buildings is

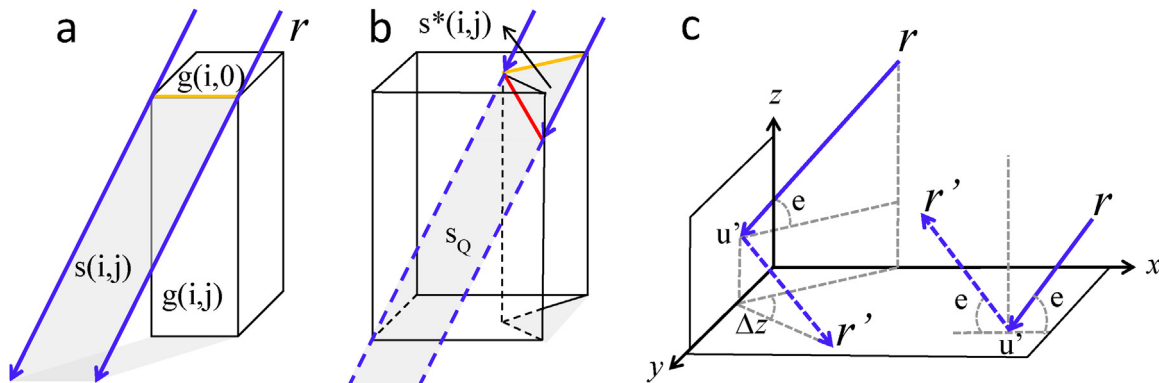
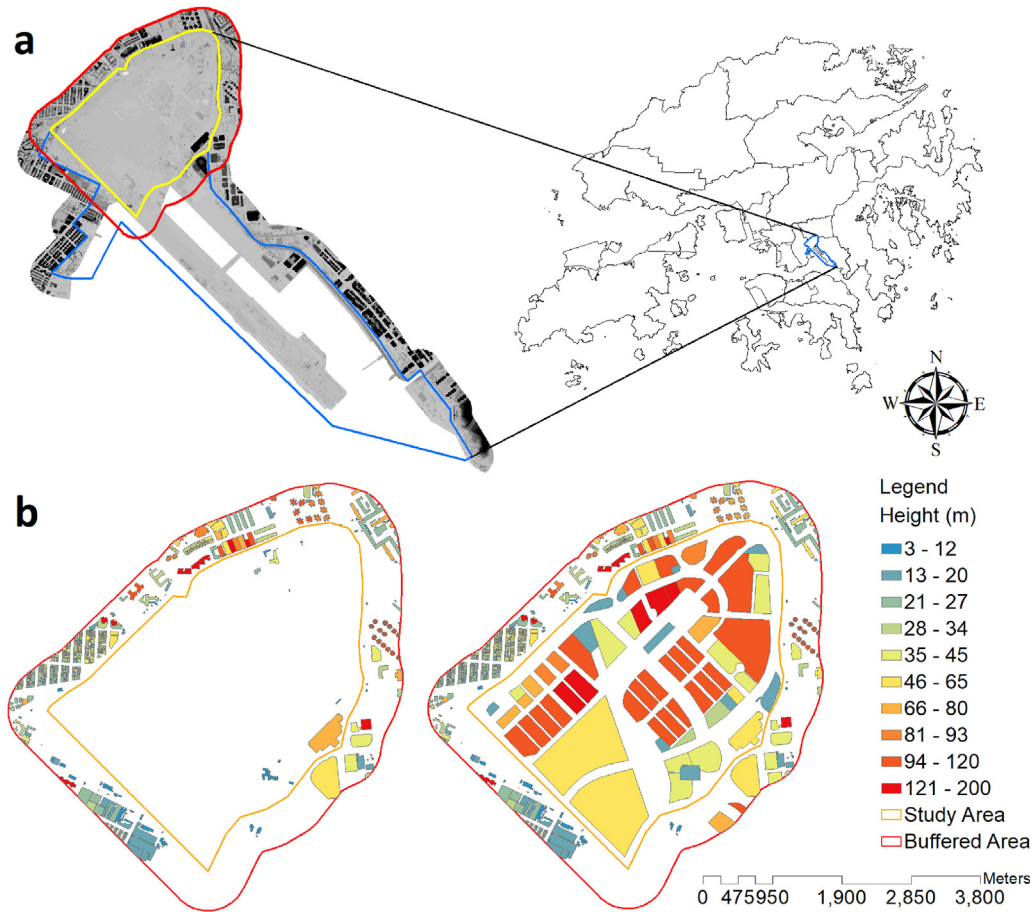


Fig. 1. Illustration for the computation of the method. (a) The shadow surface $s(i, j)$ created by two parallel solar radiation lines. (b) The modified shadow $s^*(i, j)$ by cutting from s_Q from the origin. (c) The received irradiation u' on urban surfaces derived from r .



significantly larger than previous studies.

5.2. Data collection

The influence of terrain variation on the distribution solar irradiations has been omitted because the study area is flat. Footprints of the existing buildings with the height attribute have been provided by the Land Department of Hong Kong, and the master plan of future buildings affiliated with the height information have been obtained from Statutory Planning Portal 2 ([Town Planning Board, 2019](#)). Thus, two data-sets in the current and future scenarios have been established with a number of 682 buildings (floor area in 263,740 m²) versus 734 buildings (floor area in 1,102,411 m²) ([Fig. 2b](#)). Sun Earth Tools ([Sun Earth Tools, 2018](#)) was used to compute elevation e and azimuth z of solar radiation r at an instant of time t and location l and Points Solar Radiation in the software of ArcGIS 10.3 was used to compute the irradiation u for a given r ([ArcGIS for Desktop, 2018](#)). Since cloud cover can significantly influence the irradiation u , historical monthly cloud-cover data between year 2015 and 2017 has been collected from World Weather Online ([World Weather Online, 2018](#)) in order to determine transmittivity and diffuse proportion more precisely, which are used to compute u .

5.3. Computation

Spatial resolution of the point clouds was 1 m for the empirical investigation, which generated more than 4.34 million and 6.52 million point-clouds for the ‘current city’ and ‘future city’, respectively. Therefore, computational cost can be extremely heavy, such as 3D intersections between \mathcal{R} and \mathcal{G} which can generate several millions of intermediate records. In order to achieve fast computation, the model

was implemented as a set of hierarchical SQL functions which were incorporated into an iterative computational framework in a spatial database management system (DBMS) of PostgreSQL 11, with the support of PostGIS 2.5 which provides a series of functions for 2D and 3D geometrical computation. DBeaver 5.3 has been utilized as an administrative and management tool for the database development. The model was executed on a Windows 10 Pro for Workstations with Intel (R) Xeon(R) Silver 4116 CPU (2.10 GHz, 24 cores, 48 processors, and 64 GB RAM).

In the DBMS architecture, several computational accelerating technologies were used, such as indexing of a geometry column recording location l in order to update $\{u\}$ in \mathcal{P} , recording large intermediate results as temporary tables in RAMs, and replacing an existing table with a new table instead of making UPDATE queries. Since PostgreSQL has not established a satisfactory parallel computational framework by calling several threads simultaneously for a single task, an easy and alternative approach is creating a set of independent databases and each database computes the model only for a specified time instant. This way, the databases can work in parallel without making any conflicts, and the total irradiation received by each point over continuous of time can be computed ultimately.

5.4. Results

5.4.1. Annual irradiations

Based on the aforementioned method, annual irradiations for the current city and future city were derived, respectively ([Fig. 3](#)). The analysis shows that the future city obtains more irradiation than the current city, although only marginally: a 0.31% increase from 3,025,433 MWh/yr up to 3,034,688 MWh/yr. What is notable here is that there is an improvement in solar accessibility anyway, which is an

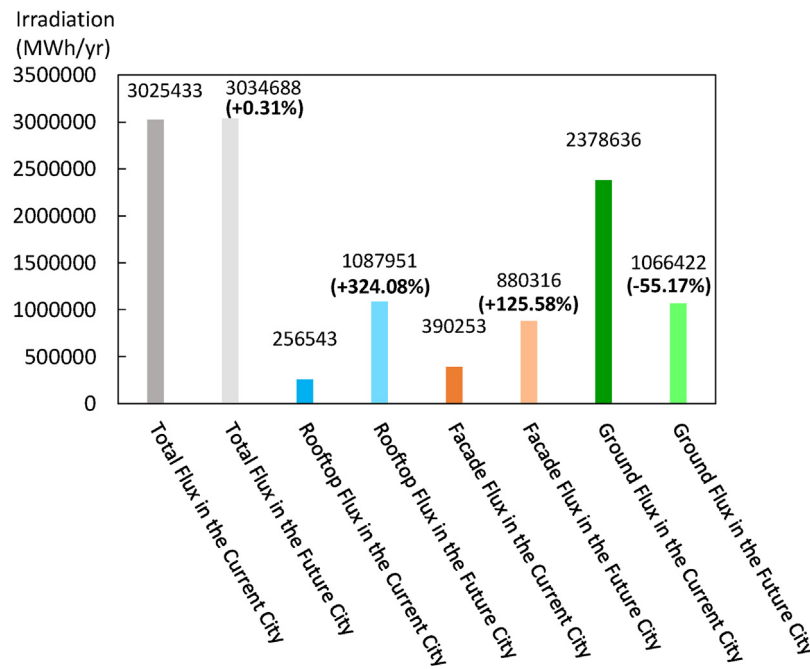


Fig. 3. Annual irradiations in the current city and the future city with their three partitions on rooftops, wall façades, and ground.

index of sustainable urban development as discussed previously. Theoretically, direct incoming solar irradiation received by a flat area is constant given the same weather condition and time period. However, if buildings located in the same flat area have larger density and heights, then more shadow areas on ground will be created, which means that these buildings could receive larger annual solar irradiations. In other words, a unit urban area with denser and higher buildings could have a higher capability to receive solar energy, depending on the urban morphology. The figure also presents that the number of the irradiation on rooftops and façades grow significantly in the future city with increases of 324.08% and 125.58% respectively because new buildings are constructed; on the contrary, solar irradiation received by ground had a dramatic drop off at 55.17%. Since majority of the irradiation is on buildings in the future city, it indicates that systematically installing photovoltaic cells on buildings is fundamental to utilize solar energy in urban areas.

5.4.2. Spatio-temporal distribution of the transformation

Citizens usually pay attention to daylighting time in their offices and accommodations throughout the year. Motivated by this, statistics in the temporal accessibility of annual solar radiation (in the x-axis)

against the percentage of urban surface area (in the y-axis) have been conducted for both the current (Fig. 4a) and the future city (Fig. 4b). Specifically, temporal accessibility is defined as the percentage of daylighting time that a unit area could obtain over an entire year. It shows that more than 50% of the total urban surface area (i.e. the sum of the pct in the y-axis) obtains more than 80% of the daylighting time (i.e. the three values larger than 0.82 in the x-axis) over the whole year for the current city (Fig. 4a), suggesting a promising urban morphology for utilizing solar energy. Both the ground curve and the overall curve have a sharp increase from 0.64 in the x-axis coincidentally, which means that the ground area makes a great contribution to the temporal accessibility because it is large and flat so that solar radiation will not be obscured by other buildings or infrastructures. However, most of the façade area can only receive solar radiation less than 55% of the total daylighting time, suggesting a neutral situation for temporal accessibility. Even though the rooftop only takes less than 5% of the total urban surface area, it has the largest temporal accessibility which is larger than 0.91 on the average.

For the future city, the ground area has an even and relatively lower distribution in a full range of temporal accessibility (Fig. 4b), which is expected given the increased built area in the future city. This

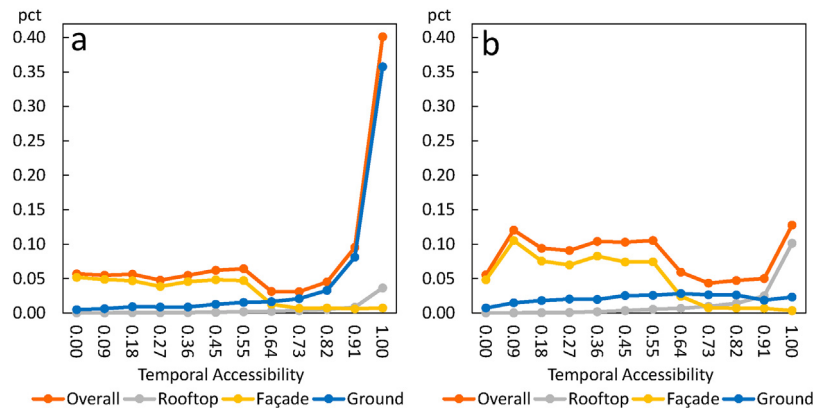


Fig. 4. Temporal accessibility of annual solar radiation (in the x-axis) against the percentage of urban surface area (in the y-axis) for the current city (a) and the future city (b) with three partitions on rooftops, wall façades, and ground.

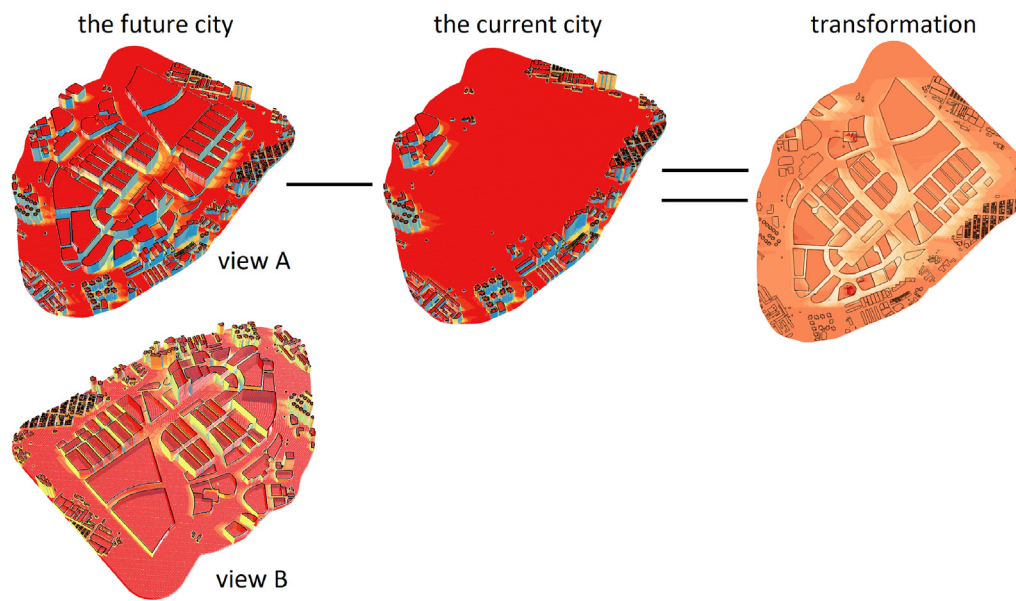


Fig. 5. Transformation of annual solar irradiations from the current city to the future city. Spatial distribution of the annual solar irradiations of the future city is visualized in view A (from north to south) and view B (from south to north). The four plots were visualized in ArcScene 10.0, where the data was exported from the database and recorded in the ESRI Shapefile format.

explanation is supported by the evidence that the rooftop area of the future city becomes larger when the temporal accessibility is larger than 0.91, which indicates a favourable potential to utilize solar energy on rooftops. In addition, the transformed temporal accessibility on ground indicates better thermal comfort routings for pedestrians since more than 50% of the ground area has a temporal accessibility smaller than 0.55. It also shows that most of the façade areas (i.e. the sum of the *pct* in the *y*-axis) have short annual daylighting time (i.e. values smaller than 0.55 in the *x*-axis), even though the façade areas in the future city are increased significantly. This may not be favourable for installing photovoltaic cells on façades, which always prefers long time of solar radiation; instead, it shall be appropriate for the daylighting purpose in offices and accommodations since most of them could have daylighting in half of the annual daytime.

In order to quantitatively investigate the changes of annual solar energy when reforming urban areas, the transformation of solar accessibility was computed by using annual solar irradiations of cloud points in the future city minus solar irradiations of the corresponding cloud points in the current city (Fig. 5). Therefore, the transformation can be organized in four categories: (i) point clouds remains on ground, (ii) point clouds originally on ground move onto new rooftops, (iii) point clouds remains on the same rooftops, and (iv) point clouds remains on the same façades. Since point clouds on façades of new buildings in the future city cannot find the corresponding point clouds in the current city, this category is thus omitted.

A number of new buildings to be built in the Kai Tak region are dense and tall, which may cause an adverse effect on the daylighting of currently existing buildings at different times of a day. To investigate this effect explicitly, the transformation of solar accessibility is plotted in three groups (increased, unchanged, and decreased) from 8 am to 6 pm on an annual-averaged day (Fig. 6). The figure shows that new buildings have effect on daylighting of south-western and northeastern buildings only at 8 am (Fig. 6a), 9 am (Fig. 6b), and 6 pm (Fig. 6k) since these buildings have decreased solar irradiations on rooftops in the three hours, while the effect is inconspicuous between 10 am (Fig. 6c) and 5 pm (Fig. 6j). Even though these buildings are affected because of the small elevation of solar radiation in the early morning and late afternoon, the effect shall be insignificant since the intensity of solar radiation in the three hours is low. In contrast, majority of the ground area between the new buildings is with the decreased solar irradiations over almost the whole daytime hours, which indicates that these locations may be under the shadow in an entire year. Notably, some areas have increased solar irradiations. It is because these areas are

transformed from the shadow on ground to brightness on rooftops, leading to a better solar accessibility, both quantitatively and temporally.

The transformation on wall façades is also presented in two views between 8 am and 1 pm, and between 2 pm and 6 pm, respectively (Fig. 7). It can be seen that the area of the decreased solar irradiations shrinks significantly for the first three hours from 8 am to 10 am, and it grows only for the last two hours from 5 pm to 6 pm. This indicates that currently existing façades will be only marginally influenced by newly constructed buildings. The above investigations suggest that new buildings to be built in the Kai Tak region will not have significant effect on the surrounding existing buildings, thanks to the appropriate choice of heights and layouts of new buildings, and the large elevations of solar radiation in Hong Kong all through a year.

5.4.3. Statistics of the transformation

Quantitative statistics of the area of transformed solar irradiations are presented to better understand the transformations (Fig. 8). The analysis shows that the area of the unchanged irradiation on ground grows from 844,385 m² at 8 am to 1,445,285 m² at 2 pm, followed by a steady decrease (Fig. 8a). As an opposite trend, the area of the decreased irradiation drops from 806,832 m² to 205,688 m² significantly from 8 am to 2 pm, followed by the other increase from 2 pm to 6 pm (Fig. 8a). The same pattern occurs in the other three categories, which, however, is not obvious for point clouds remaining on the same rooftops (Fig. 8b) and façades (Fig. 8d). Moreover, the area of the increased irradiation of point clouds remaining on ground, rooftops, and façades is small, each of which is smaller than 500 m². It is because a few nearby buildings are replaced with bare land or new buildings with lower heights so that these point clouds are transformed from under the shadow to brightness in certain time periods. In comparison, the area of the increased irradiation on new rooftops is much larger (Fig. 8c), and its curve experiences a solid decrease and increase during the daytime.

While the analysis reported previously focused on the area affected by transformation, Fig. 9 reports the amount of the increased and decreased solar irradiations. Since the amount of the unchanged irradiation is always 0, this scenario is not considered. Overall, the amounts of the increased and decreased irradiations are decreasing over the daytime, indicating that the morning hours could be the most influential time. The largest amount of the decrease occurs on ground, reaching up to 84,893 MWh/yr at 10 am (Fig. 9a), while the largest amount of the increase happens on new rooftops, arriving at 7481 MWh/yr at 8 am (Fig. 9c). In addition, transformations on the same rooftops (Fig. 9b)

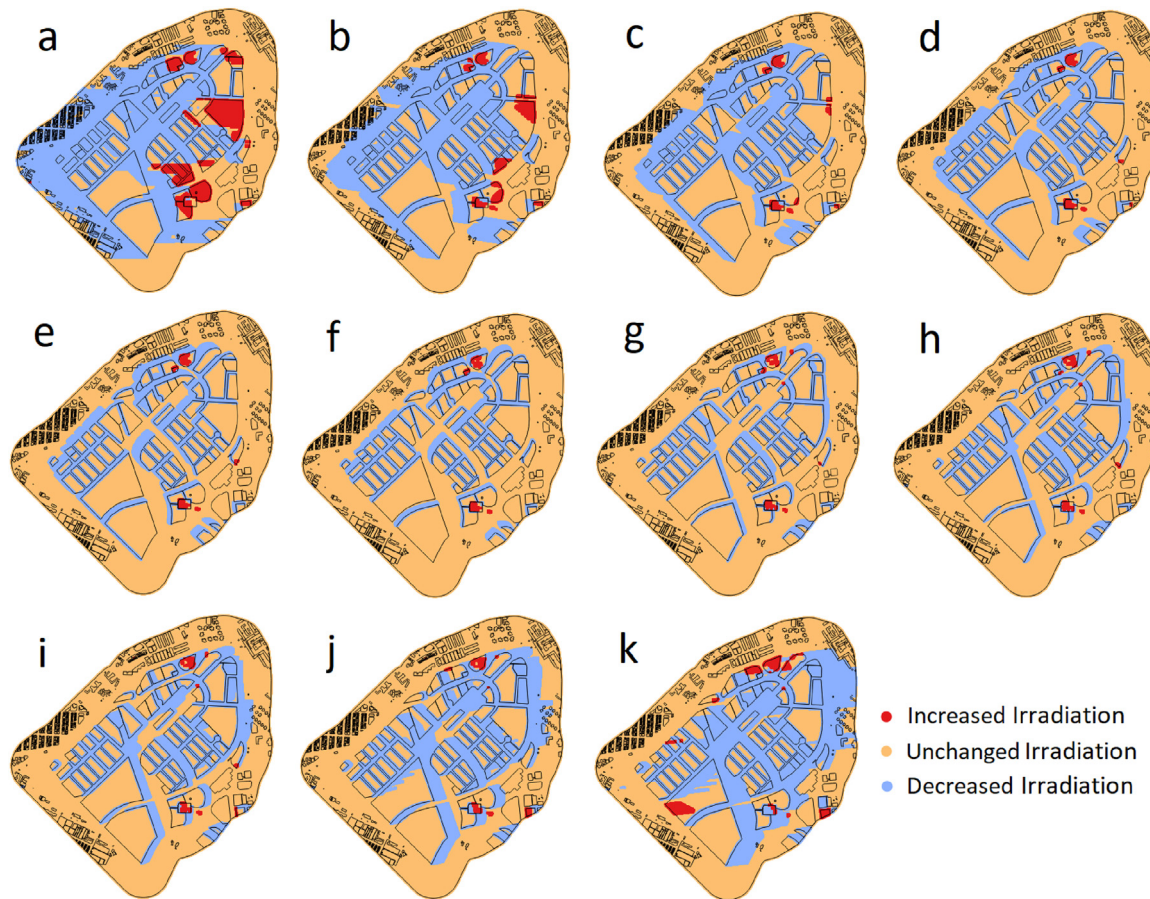


Fig. 6. Locations of transformed solar irradiations on rooftops and on ground in the future city, which compares the future city (which contains currently existing buildings and newly constructed buildings) with the current city. Plots from (a) to (k) visualize the transformation from 8 am to 6 pm on an annual-averaged day. The plots were visualized in QGIS 2.8.2, where the data was read from the database directly through the DB Manager which provides database connections.

and façades (Fig. 9d) are insignificant, indicating a marginal effect of the new development on existing buildings. This result is especially important as it provides a good argument for increasing acceptance of new development by current population. Specifically, since the notable increase of the irradiation (Fig. 9c) corresponds to a few spatially-concentrated areas on new rooftops (Fig. 6), these reformed areas may be considered further as potential locations for several solar applications, such as installing photovoltaic cells.

5.4.4. Annual transformation

Transformations of solar irradiations over an entire year are accumulated in three partitions for both the current city and future city ultimately (Fig. 10). The analysis shows that the increased irradiation dominantly occurs on new rooftops with 14,378 MWh/yr in 136,421 m², and the largest decrease irradiation is on ground with 439,318 MWh/yr in 1,138,218 m², which obtains 0.1054 MWh/yr/m² for the increase on new rooftops versus 0.3860 MWh/yr/m² for the decrease on ground averagely. Therefore, it suggests that the solar accessibility on ground is mostly affected. Notably, new rooftops obtain the second largest decrease with 273,706 MWh/yr (0.1940 MWh/yr/m²), while the decrease on existing rooftops is 63,050 MWh/yr (0.0744 MWh/yr/m²). This means that new rooftops will be affected considerably by shadows of new buildings. Furthermore, only 11.03% of the existing façades will be affected (i.e. where solar irradiations are decreased), which suggests that new buildings will not make significant effect to the daylighting of the current buildings quantitatively over the whole year.

6. Discussion and conclusion

This study can promote the integration of photovoltaic cells in an urban environment, which is not only on ground, but also on rooftops and façades of buildings. At each specific location, the amount of the electricity can be estimated based on annual solar irradiation and a reasonable photoelectric conversion efficiency (e.g., 20–25%), so that economically profitable locations can be determined, having considered the material cost, installation cost, and maintenance cost. Since some building surfaces are equipped with large area of glasses or mirrors with high albedo, some areas may be solar accumulative for a time period, benefiting from reflective irradiations from different surfaces. In this scenario, the generated electricity could be higher than expected and indoor environment could cool down consequently, leading to less use of air conditioners.

This study used officially released master plan to evaluate solar accessibility in developing cities. Alternatively, it can also contribute to urban design, supporting planners and architects in a pre-design phase. Assuming that landscape of an urban area is reformed, a demand-driven analysis can predict various usable locations, e.g., photovoltaic cells are on solar abundant façades, greenery area or urban farming are on solar modest rooftops, and sidewalk is on ground with long-term shadow. Then, an optimal master plan can be proposed for further consideration by comparing a series of different initiatives.

In a broader perspective, this study can promote the concept of the sustainable city, which brings impacts on society, economy, and environment. More specifically, the proposed method can be used for energy planning. For example, electricity generated on building surfaces could reduce its dependence on national grid, which is economic

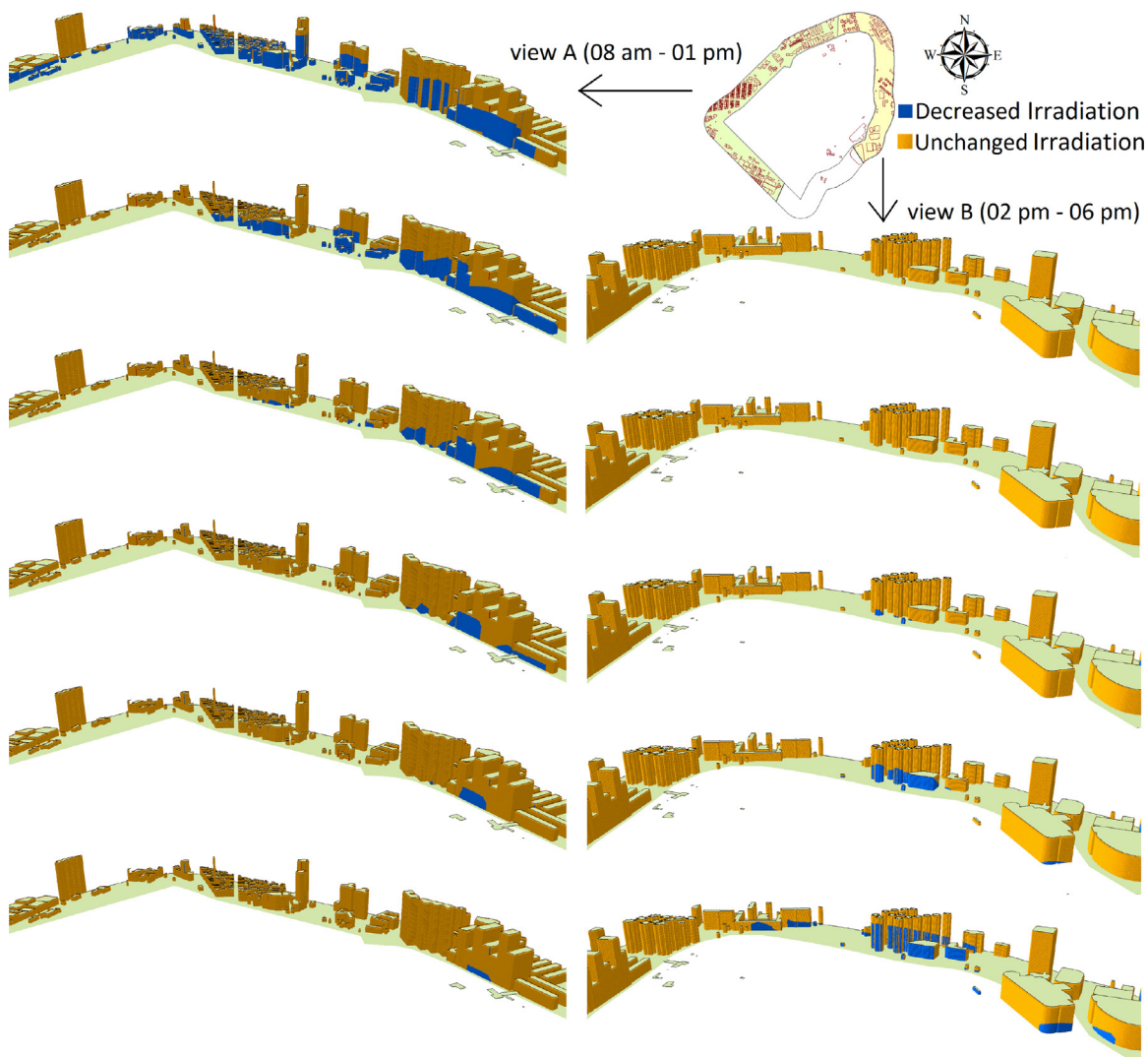


Fig. 7. Locations of transformed solar irradiations on the façades of the future city (which only contains currently existing buildings) in the 200 m buffered area. From top to bottom, it changes from 8 am to 1 pm in view A in the left side and from 2 pm to 6 pm in view B in the right side, on an annual-averaged day. The plots were visualized in ArcScene 10.0, where the data was exported from the database and recorded in the ESRI Shapefile format.

and environmental protection. Still taking photovoltaic cells for illustration, solar charging platforms used as dock stations of shared e-scooters could provide battery charging service when they are not in use during the daytime. This approach could significantly reduce the repositioning cost that logistical vehicles have to carry e-scooters back and forth for indoor battery charging. All these rely on stations having abundant solar energy and the method used this study could provide the solar-oriented site selection consultation, which shows the impacts not only on economy and environment but also on society and urban mobility.

This study estimated annual solar irradiations on a city envelope including all the rooftops, wall façades, and ground, which are represented as millions of 3D point clouds. Instead of focusing on spatio-temporal distribution of annual irradiations on the current and future city, or proposing optimal geometries of buildings, this study focuses on the transformation of solar accessibility over different time of a day and over different partitions of an urban area, in order to evaluate the effect of a determined master plan. Several conclusions can be drawn from this study:

1. The model is physically and mathematically reliable having considered some influential factors, such as monthly cloud cover, various geometries of buildings, and shadow effects made by nearby

buildings.

2. The model could compute a large urban area containing several hundreds of buildings, which is competitive compared with other models, even though it has not established a robust parallel computational framework.
3. Annual solar accessibility is affected insignificantly on existing buildings, which is mainly because of the appropriate heights of the planned buildings and annually large elevations of the direct solar radiation in Hong Kong.
4. Annual solar accessibility in the planned area is considerable and is increased when part of the ground transforms to new rooftops, but decreased on the remaining ground surface, which becomes street canyon between new buildings.

The model can be improved in three aspects. First, including reflective radiation into the global solar radiation since albedos are high on certain urban surfaces, which could produce irradiation accumulation. Second, considering terrain and greenery effects when creating 3D shadow surfaces, which could make it more applicable in other cities. Third, integrating the model into a parallel computational framework for city-scale computation.

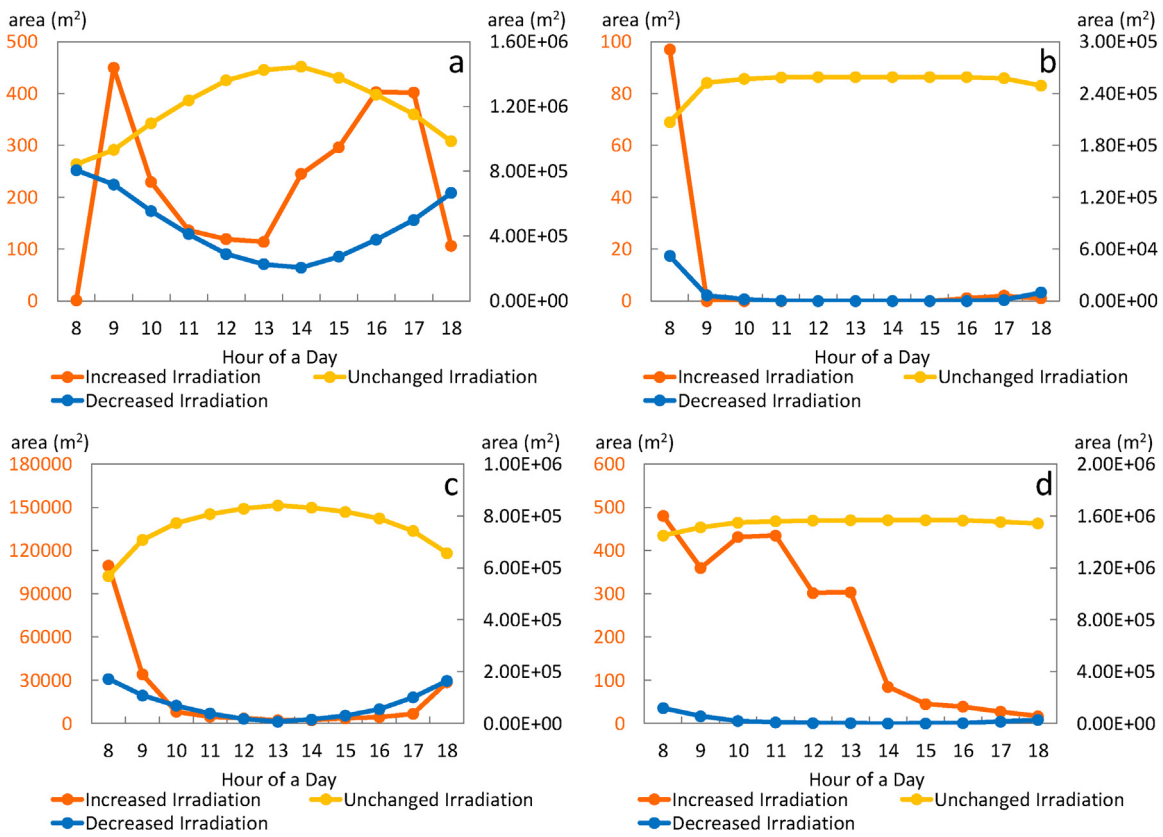


Fig. 8. The total area of transformed solar irradiations on exterior urban surfaces of the whole study area, from 8 am to 6 pm on an annual-averaged day. The left y-axis corresponds to the increased irradiation, and the right y-axis corresponds to the unchanged and decreases irradiations. (a) Point clouds remain on ground. (b) Point clouds remain on the same rooftops. (c) Point clouds move from ground to rooftops of newly constructed buildings. (d) Point clouds remain on the same façades.

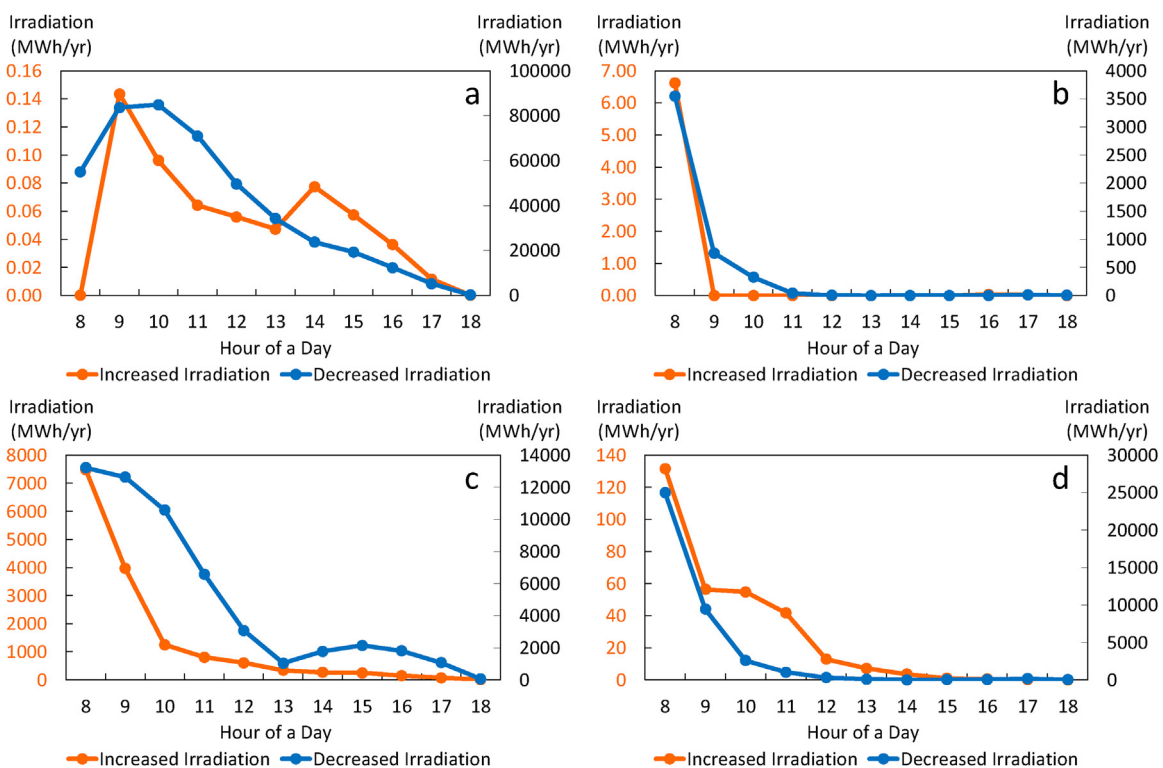


Fig. 9. The amount of transformed solar irradiations on exterior urban surfaces of the whole study area, from 8 am to 6 pm on an annual-averaged day. The left and right y-axis correspond to the increased and decreased irradiation, respectively. (a) Point clouds remain on ground. (b) Point clouds remain on the same rooftops. (c) Point clouds move from ground to rooftops of newly constructed buildings. (d) Point clouds remain on the same façades.

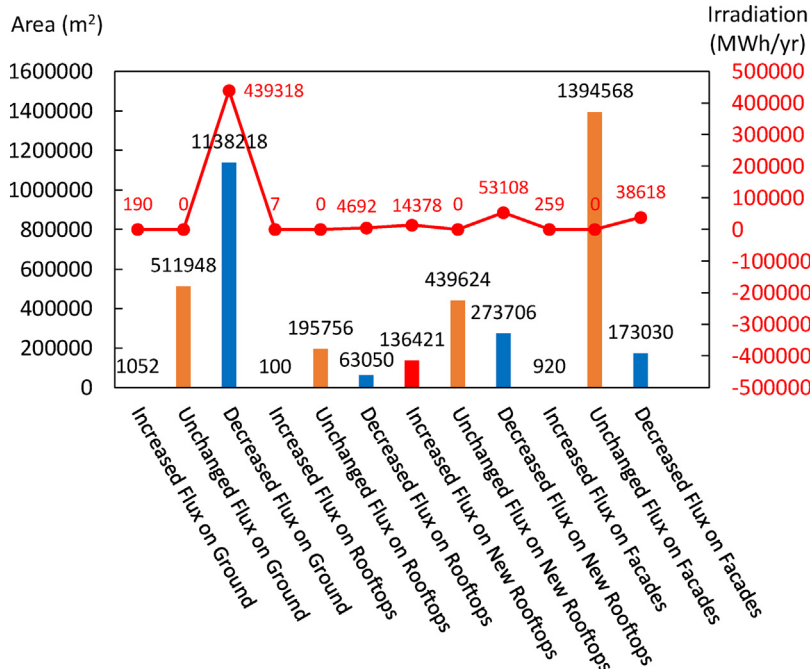


Fig. 10. The amount of transformed solar irradiations on exterior urban surfaces of the whole study area, from 8 am to 6 pm in the daytime over the whole year. The y-axis on the left side is for the bars, and the y-axis in the right side is for the red curve. (For interpretation of the references to color in this figure legend, the reader is referred to the web version of this article.)

Acknowledgements

The authors thank the support from National Research Foundation Singapore, Singapore-MIT Alliance for Research and Technology, and MIT Senseable City Laboratory. The authors also thank the Hong Kong Lands Department for the 3D building data provided.

References

- Aflaki, A., Mirnezhad, M., Ghaffarianhoseini, A., Ghaffarianhosseini, A., Omrany, H., Wang, Z. H., et al. (2017). Urban heat island mitigation strategies: A state-of-the-art review on Kuala Lumpur, Singapore and Hong Kong. *Cities*, 62, 131–145.
- Amado, M., & Poggi, F. (2014). Solar urban planning: A parametric approach. *Energy Procedia*, 48, 1539–1548.
- Amado, M., Poggi, F., & Amado, A. R. (2016). Energy efficient city: A model for urban planning. *Sustainable Cities and Society*, 26, 476–485.
- ArcGIS for Desktop (2018). Points solar radiation. Accessed 07.12.18 <http://desktop.arcgis.com/en/arcmap/10.3/tools/spatial-analyst-toolbox/points-solar-radiation.htm>.
- Atitá, C., Redweik, P., Pereira, J., & Brito, M. C. (2014). Extending solar potential analysis in buildings to vertical facades. *Computers & Geosciences*, 66, 1–12.
- Chatzipoulka, C., Compagnon, R., & Nikolopoulou, M. (2016). Urban geometry and solar availability on facades and ground of real urban forms: Using London as a case study. *Solar Energy*, 138, 53–66.
- Chu, S., & Majumdar, A. (2012). Opportunities and challenges for a sustainable energy future. *Nature*, 488, 294–303.
- Development Bureau (2019). The HKSAR Government. Energizing Kowloon East. Accessed 29.01.19 <https://www.ecko.gov.hk/en/home/index.html>.
- Erdélyi, R., Wang, Y., Guo, W., Hanna, E., & Colantuono, G. (2014). Three-dimensional Solar Radiation Model (SORAM) and its application to 3-D urban planning. *Solar Energy*, 101, 63–73.
- GEA Writing Team (2012). Global energy assessment – Toward a sustainable future. Cambridge, UK and New York, NY, USA/Laxenburg, Austria: Cambridge University Press/International Institute for Applied Systems Analysis.
- Gong, F. Y., Zeng, Z. C., Ng, E., & Norford, L. K. (2019). Spatiotemporal patterns of street-level solar radiation estimated using Google Street View in a high-density urban environment. *Built and Environment*, 148, 547–566.
- Hofierka, J., & Zloch, M. (2012). A new 3-D solar radiation model for 3-D city models. *Transactions in GIS*, 16(5), 681–690.
- IZquierdo, S., Montañés, C., Dopazo, C., & Fueyo, N. (2011). Roof-top solar energy potential under performance-based building energy codes: The case of Spain. *Solar Energy*, 85(1), 208–213.
- Jakubiec, J. A., & Reinhart, C. F. (2013). A method for predicting city-wide electricity gains from photovoltaic panels based on LiDAR and GIS data combined with hourly Daysim simulations. *Solar Energy*, 93, 127–143.
- Kanters, J., Wall, M., & Dubois, M. C. (2014). Typical values for active solar energy in urban planning. *Energy Procedia*, 48, 1607–1616.
- Lauka, D., Haine, K., Gusca, J., & Blumberga, D. (2018). Solar energy integration in future urban plans of the South and Nordic cities. *Energy Procedia*, 152, 1127–1132.
- Li, Y., Ding, D., Liu, C., & Wang, C. (2016). A pixel-based approach to estimation of solar energy potential on building roofs. *Energy and Buildings*, 129, 563–573.
- Liang, J., Gong, J., Li, W., & Ibrahim, A. N. (2014). A visualization-oriented 3D method for efficient computation of urban solar radiation based on 3D–2D surface mapping. *International Journal of Geographical Information Science*, 28(4), 780–798.
- Liang, J., Gong, J., Zhou, J., Ibrahim, A. N., & Li, M. (2015). An open-source 3D solar radiation model integrated with a 3D Geographic Information System. *Environmental Modelling & Software*, 64, 94–101.
- Lindberg, F., Jonsson, P., Honjo, T., & Wästberg, D. (2015). Solar energy on building envelopes – 3D modelling in a 2D environment. *Solar Energy*, 115, 369–378.
- Lin, H., Chen, M., Lu, G., Zhu, Q., Gong, J., You, X., et al. (2013). Virtual geographic environments (VGEs): A new generation of geographic analysis tool. *Earth-Science Reviews*, 126, 74–84.
- Lobaccaro, G., & Frontini, F. (2014). Solar energy in urban environment: How urban densification affects existing buildings. *Energy Procedia*, 48, 1559–1569.
- Lobaccaro, G., Carlucci, S., Croce, S., Paparella, R., & Finocchiaro, L. (2017). Boosting solar accessibility and potential of urban districts in the Nordic climate: A case study in Trondheim. *Solar Energy*, 149, 347–369.
- Lu, G., Batty, M., Strobl, J., Lin, H., Zhu, A. X., & Chen, M. (2019). Reflections and speculations on the progress in Geographic Information Systems (GIS): A geographic perspective. *International Journal of Geographical Information Science*, 33(2), 346–367.
- Ma, S., Goldstein, M., Pitman, A. J., Haghdi, N., & MacGill, I. (2017). Pricing the urban cooling benefits of solar panel deployment in Sydney, Australia. *Scientific Reports*, 7, 43938.
- Masson, V., Bonhomme, M., Salagnac, J. L., Briottet, X., & Lemonsu, A. (2014). Solar panels reduce both global warming and urban heat island. *Frontiers in Environmental Science*, 2, 14.
- Middel, A., Lukasczyk, J., & Maciejewski, R. (2017). Sky view factors from synthetic fisheye photos for thermal comfort routing - A case study in Phoenix, Arizona. *Urban Planning*, 2(1), 19–30.
- Molina, A., Falvey, M., & Rondanelli, R. (2017). A solar radiation database for Chile. *Scientific Reports*, 7, 14823.
- Morganti, M., Salvati, A., Coch, H., & Cecere, C. (2017). Urban morphology indicators for solar energy analysis. *Energy Procedia*, 134, 807–814.
- Nastasi, B., & Di Matteo, U. (2016). Solar energy technologies in Sustainable Energy Action Plans of Italian big cities. *Energy Procedia*, 101, 1064–1071.
- Perez, R., Ineichen, P., Seals, R., Michalsky, J., & Stewart, R. (1990). Modeling daylight availability and irradiance components from direct and global irradiance. *Solar Energy*, 44(5), 271–289.
- Peronato, G., Rey, E., & Andersen, M. (2018). 3D model discretization in assessing urban solar potential: The effect of grid spacing on predicted solar irradiation. *Solar Energy*, 176, 334–349.
- Planning Department (2017). The HKSAR Government. Land utilization in Hong Kong. Accessed 29.01.19 https://www.pland.gov.hk/pland_en/info_serv/statistic/landu.html.
- Polo L'peza, C. S., Salab, M., Tagliabuec, L. C., Frontinia, F., & Bouziri, S. (2016). Solar radiation and daylighting assessment using the Sky-View Factor (SVF) analysis as method to evaluate urban planning densification policies impacts. *Energy Procedia*, 91, 989–996.
- Poruschi, L., & Ambrey, C. L. (2019). Energy justice, the built environment, and solar photovoltaic (PV) energy transitions in urban Australia: A dynamic panel data analysis. *Energy Research & Social Science*, 48, 22–32.

- Redweik, P., Catita, C., & Brito, M. (2013). Solar energy potential on roofs and facades in an urban landscape. *Solar Energy*, *97*, 332–341.
- Savvides, A., Vassiliades, C., Michael, A., & Kalogirou, S. (2019). Siting and building-massing considerations for the urban integration of active solar energy systems. *Renewable Energy*, *135*, 963–974.
- Sun Earth Tools (2018). *Tools for consumers and designers of solar*. Accessed 07.12.18 https://www.sunearthtools.com/dp/tools/pos_sun.php?lang=en.
- Town Planning Board (2019). *statutory planning portal 2*. Accessed 29.01.19 <https://www2.ozp.tpb.gov.hk/gos/default.aspx>.
- Vakilifard, N., Bahri, P. A., Anda, M., & Ho, G. (2019). An interactive planning model for sustainable urban water and energy supply. *Applied Energy*, *235*, 332–345.
- Wong, M. S., Zhu, R., Liu, Z., Lu, L., Peng, J., Tang, Z., et al. (2016). Estimation of Hong Kong's solar energy potential using GIS and remote sensing technologies. *Renewable Energy*, *99*, 325–335.
- Wong, I. L. (2017). A review of daylighting design and implementation in buildings. *Renewable and Sustainable Energy Reviews*, *74*, 959–968.
- World Weather Online (2018). *Historical monthly weather*. Accessed 07.12.18 <https://www.worldweatheronline.com>.